



Texture analysis of deep medullary veins on susceptibility-weighted imaging in infants: evaluating developmental and ischemic changes

Hyun Gi Kim^{1,2} · Jin Wook Choi² · Miran Han² · Jang Hoon Lee³ · Hye Sun Lee⁴

Received: 20 August 2019 / Revised: 7 November 2019 / Accepted: 11 December 2019 / Published online: 5 February 2020
© European Society of Radiology 2020

Abstract

Objective Susceptibility-weighted imaging (SWI) can be used to evaluate deep medullary veins (DMVs). This study aimed to apply texture analysis on SWI to evaluate developmental and ischemic changes of DMV in infants.

Methods A total of 38 infants with normal brain MRI (preterm [$n = 12$], term-equivalent age [TEA] [$n = 18$], and term [$n = 8$]) and seven infants with ischemic injury (preterm [$n = 2$], TEA [$n = 1$], and term [$n = 4$]) were included. Regions of interests were manually drawn to include DMVs. First-order texture parameters including entropy, skewness, and kurtosis were derived from SWI. The parameters were compared between groups according to age and presence of ischemic injury. A regression analysis was performed to correlate postmenstrual age (PMA) and parameters. A ROC analysis was performed to differentiate ischemic infants from normal infants.

Results Among parameters, entropy showed a significant difference between the age groups (preterm vs. TEA vs. term; 5.395 vs. 4.885 vs. 4.883, $p = 0.001$). There was a significant positive relationship between PMA and entropy (R square = 0.402, $p < 0.001$). Skewness was significantly higher in the ischemic group compared with that in the normal group (1.37 vs. 0.70, $p = 0.001$). The ROC on skewness resulted in an AUC of 0.87 (accuracy, 83.2%) for differentiating infants with ischemic injury.

Conclusion A texture analysis of DMVs on SWI showed differences according to age and presence of ischemic injury. The texture parameters can potentially be used as quantitative markers for differentiating infants with ischemic injury through DMV changes.

Key Points

- The DMV structure of the infant brain could be quantified on SWI with texture analysis.
- Entropy from texture analysis on SWI increased as infants got older.
- Normal and ischemic injured infants could be differentiated with a cutoff value of 1.025 for skewness.

Keywords Magnetic resonance imaging · Infant · Brain · Quantitative evaluation · Radiomics

Hyun Gi Kim and Jin Wook Choi contributed equally to the study and share first authorship.

Electronic supplementary material The online version of this article (<https://doi.org/10.1007/s00330-019-06618-6>) contains supplementary material, which is available to authorized users.

✉ Hyun Gi Kim
catharina@catholic.ac.kr

¹ Department of Radiology, Eunpyeong St. Mary's Hospital, College of Medicine, The Catholic University of Korea, Seoul, Republic of Korea

² Department of Radiology, Ajou University School of Medicine, Ajou University Medical Center, Suwon, Republic of Korea

³ Department of Pediatrics, Ajou University School of Medicine, Ajou University Medical Center, Suwon, Republic of Korea

⁴ Biostatistics Collaboration Unit, Yonsei University College of Medicine, Seoul, Republic of Korea

Abbreviations

AUC	Area under the curve
CI	Confidence interval
DMV	Deep medullary vein
DTI	Diffusion tensor imaging
DWI	Diffusion-weighted imaging
ICC	Interclass correlation coefficient
MRI	Magnetic resonance imaging
PMA	Postmenstrual age
ROC	Receiver operating characteristic curve
ROI	Region of interest
SWI	Susceptibility-weighted imaging
T1WI	T1-weighted imaging
T2WI	T2-weighted imaging
TEA	Term-equivalent age
WM	White matter

Introduction

Brain magnetic resonance imaging (MRI) has become the modality of choice for examining normal brain maturation, neonatal brain injury, and developmental neurological disorder [1]. In premature infants, white matter (WM) is the main focus of brain injuries [2]. Term infants with hypoxic-ischemic injury can also show isolated WM lesions [3, 4]. Among brain MRI sequences, susceptibility-weighted imaging (SWI) has been developed and increasingly applied in clinical practice for MRI. The SWI sequence is sensitive to susceptibility changes such as hemorrhage and calcifications [5, 6]. This relatively new technique allows visualization of the deep medullary vein (DMV) in infants [7].

DMV engorgement is often observed in infants using SWI and has been associated with periventricular hemorrhagic infarction [8] and ischemia [9]. DMV prominence has not only been associated with sinovenous thrombosis, but with WM lesions in infants [7]. In hypoxic conditions, the DMV is more prominent due to decreased oxygenation in the veins [10]. Although DMV engorgement is thought to be a pathologic change observable with SWI, no objective method has been used to quantify this prominence in past research.

Currently, texture analysis can reveal tissue characteristics with image parameters. For instance, kurtosis describes the peakedness of a signal intensity histogram, entropy describes the heterogeneity of an image, and skewness describes the average brightness of highlighted features. These parameters quantitatively show characteristics which were not previously discernible via simple visual analysis. There have been attempts to apply texture analysis on brain MRI to quantitatively show tissue characteristics of brain tumors with diffusion-weighted imaging (DWI) [11] or other conventional sequences [12, 13]. To quantify DMVs, another study tried to count and compute venous density with 7-T brain MRI [14].

In that study, DMVs were assessed and quantified with automatically created region of interests (ROIs) close to the lateral ventricles [14].

It is important to assess DMV prominence in infants since it is related to pathologic conditions such as ischemia. A recent study suggested a visual scoring system for WM injury after DMV thrombosis [15]. However, to the best of our knowledge, there have been no previous reports quantitatively examining DMV prominence. We hypothesized that SWI textural analysis parameters could help radiologists quantitatively compare DMVs in infants. To test this hypothesis, we compared SWI texture parameters by age group and showed relationships with postmenstrual age (PMA). We also compared SWI texture parameters between infants with normal MRI and infants with ischemic injury.

Materials and methods

Patients

This retrospective study was approved by our institutional review board, which waived written informed consent for the review of medical records and images. The inclusion criteria were as follows: (1) infants who were admitted to our hospital's neonatal intensive care unit, (2) infants who underwent brain MRI with a 3-T scanner (MR 750w, GE Healthcare) from December 2017 to December 2018, (3) infants with MRI including SWI, (4) infants who were either born preterm (gestational age < 37 weeks) or term (gestational age 37 weeks and older), and (5) infants with a PMA of less than 6 months. Exclusion criteria were as follows: (1) infants with intracranial hemorrhage; (2) infants with congenital malformations, infection, or metabolic disease; and (3) infants with motion artifacts on MRI. We excluded infants with intracranial hemorrhage as we wished to quantify the degree of DMV prominence and not definite hemorrhage that would affect texture parameters on SWI.

First, the infants were grouped according to age. The preterm infants were divided into two age groups, infants who underwent MRI at preterm and those who underwent MRI at term-equivalent age (TEA). The term infants were defined as the term age group. Demographic information was collected by reviewing medical records. Next, by reviewing MRI, the infants were grouped according to their MRI findings. The normal group consisted of infants without abnormalities observed on brain MRI and the ischemic group consisted of infants with ischemic injury. As the brain matures the fastest in infancy, which is reflected in its rapid tissue changes [16], we evaluated texture parameters according to PMA in infants. Relationships between PMA and texture parameters were evaluated in the normal group. As our study population included patients of a large age range, we further evaluated the

relationships between PMA and texture parameters after excluding infants who were 400 days or older. Ischemic injury was indicated on MRI by “diffusion restriction in thalami, basal ganglia, cortical, or subcortical WM,” “periventricular WM injury with high signal intensity lesions on T1-weighted image (T1WI),” or “DMV engorgement” [7, 17]. A pediatric radiologist with 9 years of experience and a neuroradiologist with 12 years of experience reviewed the MRI and confirmed the findings in each group.

MRI imaging acquisition

During the study period, the routine MRI protocols included the 3D T1WI fast spoiled gradient-echo sequence, axial T2-weighted image (T2WI), and SWI. The parameters for 3D T1WI fast spoiled gradient-echo were field-of-view 220×220 mm; slice thickness 1 mm; TR/TE 9/3 ms; and NEX 1. The parameters for T2WI were field-of-view 180×180 mm; slice thickness 3 mm; TR/TE 6000/151 ms; and NEX 2. The parameters for SWI were field-of-view 160×200 mm; $0.9 \times 0.5 \times 2$ mm³ voxel size; TR/TE = 47/23 ms; and flip angle = 15°. Axial minimum intensity projection was performed with 5-mm thickness and 2.5-mm spacing.

Texture analysis

Texture analysis was performed on WM with DMVs. MR images were moved to a computer and analyzed using the texture analysis software, TexRAD. ROIs were drawn at the right and left WM involving the DMV. We selected one axial slice to draw the ROI on at the level where the DMV showed its typical fan pattern of drainage into the subependymal vein. Each slice was chosen by each observer independently. We excluded large cortical veins and subependymal veins when drawing the ROI. The details of texture analysis are provided in Supplementary material (S1). A spatial scale filter value of 2 mm was selected for the fine texture scale among spatial scale filter values (2–6 mm) [18]. The spatial scale filter value refers to the radius of the highlighted features. Since the DMVs are fine structure with a small diameter, we chose a 2-mm spatial scale filter over spatial scale filters with larger values. Using the filtered images, heterogeneity within the ROIs was quantified with the following parameters: entropy, skewness, and kurtosis (Appendix).

Reproducibility

Intra- and inter-observer reproducibility was evaluated for the texture parameters. Two observers performed the ROI analysis. Observer 1 was a researcher with 4 years of experience in the radiology department and 2 years of experience in neuroimaging. Observer 2 was a pediatric radiologist with 9 years of experience in neuroimaging. Observer 1 drew ROIs for all

subjects and repeated the measurements for 20 subjects. The first and second measurements were compared to evaluate intra-observer reproducibility. To evaluate inter-observer reproducibility, observer 2 drew ROIs for 20 subjects and the resulting texture parameter values were compared with those of observer 1.

Statistics

The independent *t* test was used to compare age between the normal and ischemic group. To compare age groups within the normal group, nonparametric statistics of Kruskal-Wallis and pairwise tests with Dunn’s post hoc and Bonferroni correction were used. In the normal group, Spearman’s test was applied to find correlations between the texture parameters and PMA. As brain developmental changes on MRI follow a logarithmic model, we applied model fitting with texture parameters that showed significant correlation on Spearman’s test [19, 20]. The Mann-Whitney *U* test was applied to compare skewness between the normal and ischemic group. Receiver operating characteristic curve (ROC) analysis was performed to compare the parameters of the normal and ischemic group. Interclass correlation coefficients (ICC) (two-way mixed-effects model, absolute agreement, average measures) were calculated for intra- and inter-observer reproducibility. A $p < 0.05$ indicated statistical significance. SPSS, version 25.0 (IBM), was used for the statistical analyses.

Results

Patients

Among 126 infants who were admitted to our neonatal intensive care unit and who underwent brain MRI during the study period, 107 had SWI and we excluded 62 infants (the details are provided in Supplementary material, S2). After exclusion, 45 infants met our study criteria. Among the 45 infants, 38 infants showed no abnormalities on brain MRI (MRI scan at preterm [$n = 12$], TEA [$n = 18$], and term [$n = 8$]) and were considered the normal group. Seven infants had ischemic injury on brain MRI (MRI scan at preterm [$n = 2$], TEA [$n = 1$], and term [$n = 4$]) and were considered the ischemic group. Demographic data of the patients are summarized in Table 1. There was no significant difference in PMA between the normal and ischemic group (285.9 ± 53.8 days vs. 269.7 ± 16.1 days, $p = 0.439$).

Comparison between age groups

Comparison of texture parameters between the three age groups is summarized in Table 2. Entropy showed a significant difference between the three groups. When the two age groups were compared, term infants showed significantly

Table 1 Demographic characteristics of the infants

	Age group	Number	PMA (days)	Corrected GA (weeks)	Postnatal age (days)	Birth weight (g)
Normal (<i>n</i> = 38)	Preterm	12	226 (9)	32	50 (16)	1175 (175)
	TEA	18	270 (23)	39	56 (28)	1345 (650)
	Term	8	286 (152)	41	11 (111)	3165 (619)
Ischemia (<i>n</i> = 7)	Preterm	2	248	35	49	1315
	TEA	1	267	38	31	1320
	Term	4	280 (8)	40	14 (32)	3093 (106)

Data are in medians (interquartile ranges); *PMA*, postmenstrual age; *GA*, gestational age; *TEA*, term-equivalent age

higher entropy compared with preterm infants (5.395 vs. 4.883, *p* = 0.003). There was no significant difference between term and TEA infants (5.395 vs. 4.885, *p* = 0.075). TEA and preterm infants showed no significant differences in entropy (4.885 vs. 4.883, *p* > 0.999). There was also no significant difference in skewness (*p* = 0.712) and kurtosis (*p* = 0.946) between the age groups.

Relationship with postmenstrual age

There was a positive relationship between PMA and entropy (logarithmic regression model, entropy = - 3.566 + 1.532 × log [PMA], R square = 0.402, *p* < 0.001) (Fig. 1). There was a negative relationship between PMA and skewness (logarithmic regression model, skewness = 12.404 + - 2.064 × log [corrected GA], R square = 0.248, *p* = 0.001). There was no significant correlation between PMA and kurtosis (*r* = 0.469, *p* = 0.469). The results of infants younger than 400 days are provided in Supplementary material (S3).

Comparison with infants with ischemia

There was significantly higher skewness in the ischemic group compared with that in the normal group (median [interquartile range], 1.37 [0.3] vs. 0.70 [0.58]; *p* = 0.001) (Fig. 2). Between the ischemic and normal group, there was no significant difference in entropy (5.260 [0.63] vs. 4.983 [0.54], *p* = 0.316) or kurtosis (3.895 [10.64] vs. 1.910 [1.93], *p* = 0.061). Compared with the normal term infants (*n* = 8), the ischemic term infants (*n* = 4) showed significantly higher skewness

(1.143 [0.27] vs. 0.690 [0.9], *p* = 0.016). Representative MRIs are shown in Figs. 3 and 4.

ROC analysis

We performed a ROC analysis of skewness to differentiate the normal and ischemic group (Fig. 5). The skewness cutoff value of 1.025 exhibited a sensitivity of 100%, specificity of 78.9%, positive predictive value of 46.7%, and negative predictive value of 100% (area under the curve [AUC] = 0.865 (0.761, 0.969), accuracy = 83.2%, *p* value for ROC curve = 0.002). (The confusion matrix is provided in Supplementary material S4).

Reproducibility

The ICC for intra-observer reproducibility was 0.984 (95% confidence interval [CI], 0.950–0.994) for entropy; 0.708 (95% CI, 0.280–0.883) for skewness; and 0.370 (95% CI, - 0.541–0.747) for kurtosis. The ICC for inter-observer reproducibility was 0.984 (95% CI, 0.928–0.995) for entropy; 0.810 (95% CI, 0.513–0.925) for skewness; and 0.189 (95% CI, -0.898–0.669) for kurtosis.

Discussion

The results of our study suggest that there was a significant difference in entropy according to age in infants. There was a positive relationship between PMA and entropy and a

Table 2 Texture parameter values according to the age groups of normal infants

Age groups	Term		TEA		Preterm		<i>p</i> value
	Median	IQR	Median	IQR	Median	IQR	
Entropy	5.395	0.355	4.885	0.533	4.883	0.32	0.001*
Skewness	0.69	0.902	0.718	0.674	0.7	0.59	0.712
Kurtosis	1.833	0.725	1.895	3.109	2.47	2.575	0.946

TEA, term-equivalent age; *IQR*, interquartile range

*Differed significantly in pairwise comparisons

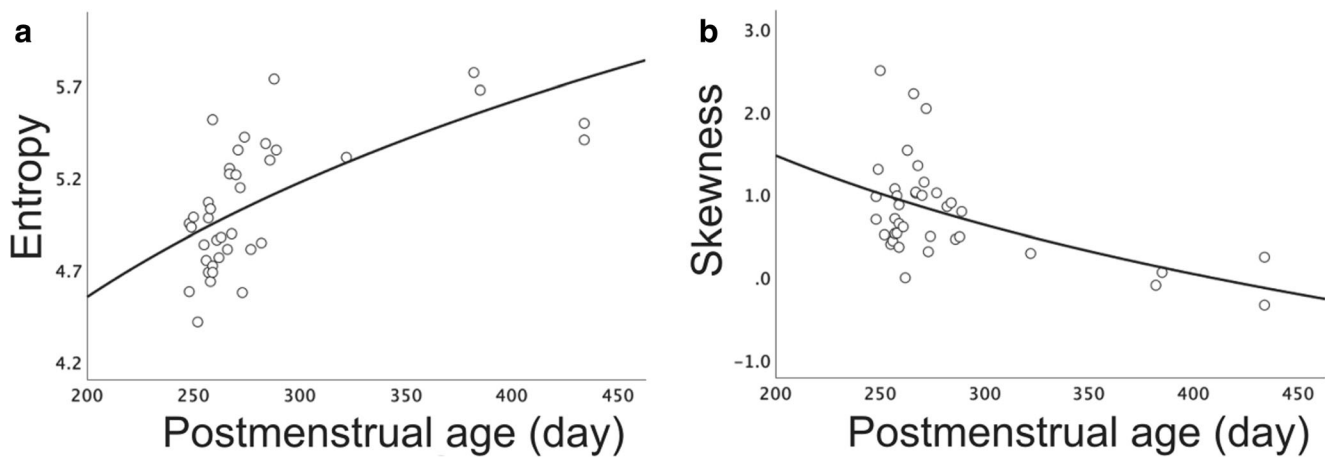


Fig. 1 Relationship between PMA and texture parameters. There is a positive relationship between PMA and entropy (a) and a negative relationship between PMA and skewness (b)

negative relationship between PMA and skewness. The diagnostic accuracy of SWI skewness was significant for differentiating ischemic injured patients. Thus, we believe that the skewness value from SWI can be used to differentiate infants with ischemic injury. Assessing the texture features of DMVs might be of clinical benefit, as they are relevant and quantifiable parameters of ischemic injuries. In addition, the texture features of the DMV could potentially reflect developmental changes. As the convergence pattern of DMVs is related to crossing nerve fiber tracts [21, 22], the texture features of DMVs might reveal an aspect of WM maturation.

In the cerebral venous system, the DMVs drain blood from the WM to the subependymal veins and has a typical fan pattern [23, 24]. This pattern is due to the anatomical distribution of the veins, which connects the subcortical WM to the ventricular surface. In infants, venous congestion occurs easily due to converging zones of veins. The linear WM lesions in preterm and full-term infants correlate with the distribution of DMVs [7, 25]. Thus, preterm and full-term infant encephalopathy is interpreted as a congestion or thrombosis of DMV.

Compared with conventional MRI sequences, SWI can better delineate cerebral venous structures in both healthy and pathologic subjects. This is because SWI is sensitive to deoxygenated blood and can show the venous drainage of DMVs as a hypointense linear structure. Cone-beam computed tomography is reported to be another imaging tool that shows fine venous angioarchitecture [26]. However, since infants are

vulnerable to radiation, using it just to evaluate DMVs is not thought suitable for the young population. Pathologic venous changes have been studied in children using SWI for conditions such as chronic ischemia [27, 28], developmental venous anomalies, microhemorrhages [29], convulsive disorder, and hypoxic-ischemic injury [30]. In a study on pediatric convulsive disorder, children who underwent SWI after their seizures showed a low cerebral vein signal [31]. This can be explained with venous pCO₂ increasing during a seizure event.

For ischemic changes, abnormal SWI hypointensity correlates with infarcted territory [27, 28] or diffuse hypoxic-ischemic conditions [30]. Studies suggest that SWI can have early predictive value, as abnormal venous structures can be revealed on SWI before abnormalities are observed on DWI [30, 31]. The DMV engorgement seen in infants with ischemic injury is thought to be responsible for WM damage which can later develop into periventricular leukomalacia [7]. Pathologically, the major findings of periventricular leukomalacia are edema and exudative hemorrhage associated with small-size coagulation necrosis.

Incorporating texture analysis to MRI has been done in other studies but mostly for tumor imaging [11, 13, 18]. Still, there have been attempts to quantify SWI to reflect cerebral hemodynamics. In a study on neonatal hypoxic-ischemic injury, DMV abnormalities were visually assigned grades from 1 to 7 [9]. The grading correlated with 6-month outcomes in infants and also correlated with the Barkovich

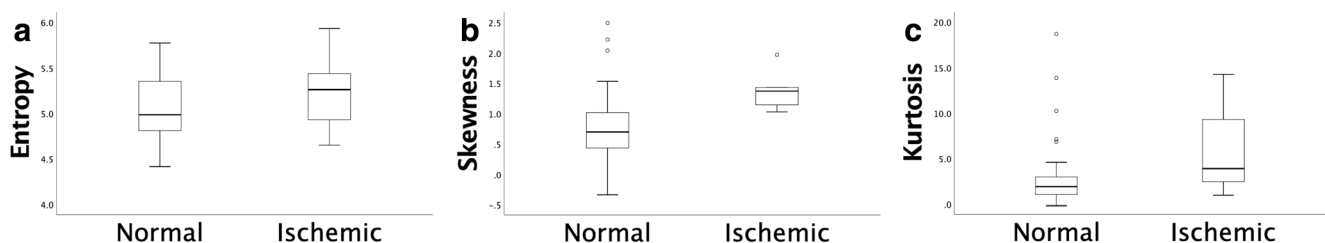


Fig. 2 Boxplot comparing texture parameters in normal and ischemic infants. Entropy (a), skewness (b), and kurtosis (c) of normal and ischemic infants

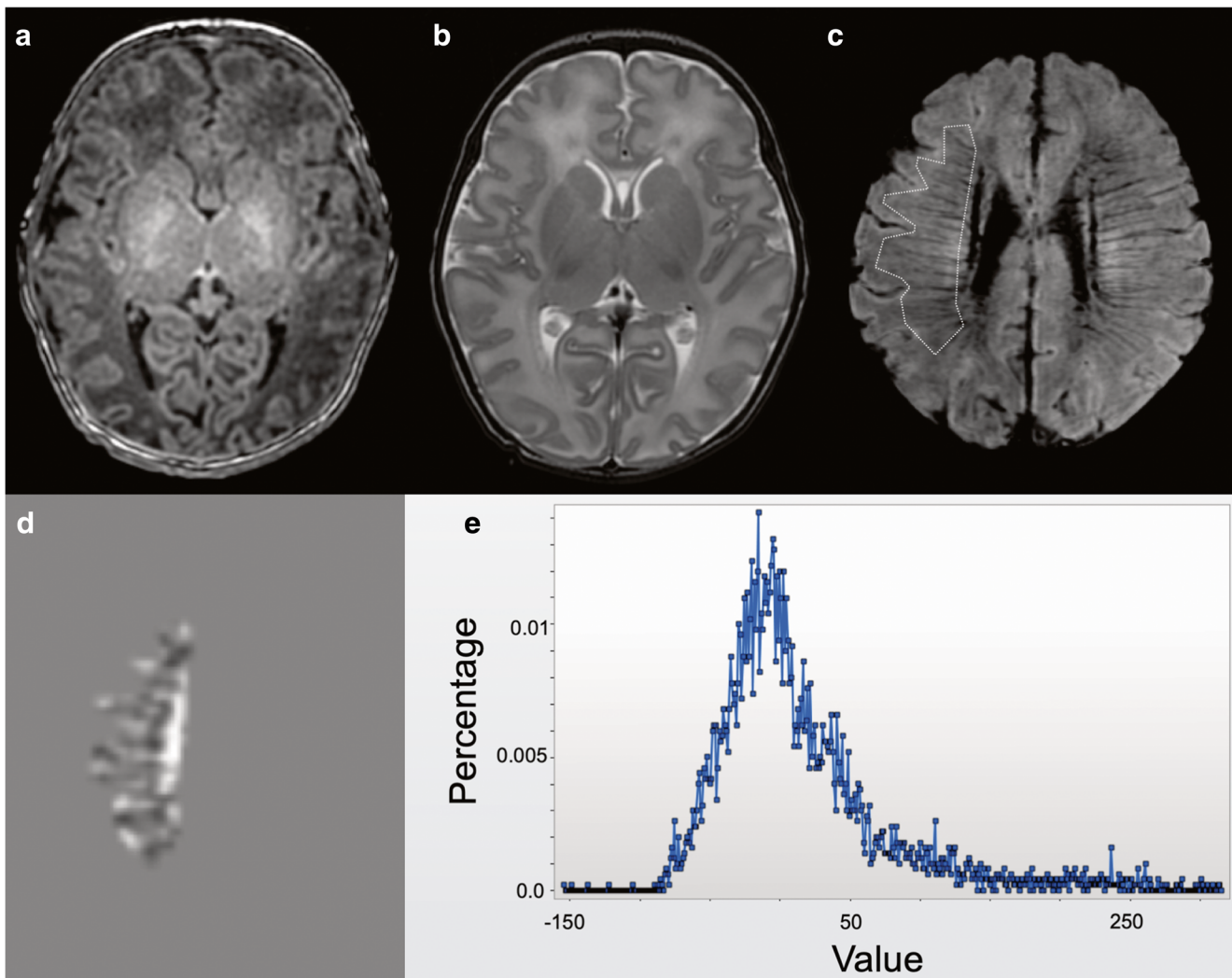


Fig. 3 A full-term infant. T1WI (a), T2WI (b), SWI (c) with ROI placement, the corresponding texture image (d), and histogram (e) of SWI

MRI scoring system [9]. In another study on pediatric arterial ischemic stroke patients, a semiquantitative analysis of venous signal intensity was done using SWI and diffusion tensor imaging (DTI) [32]. In that study, mismatches between SWI and DTI predicted the progression of ischemic stroke in patients [32]. Although studies on SWI have shown that it can demonstrate injured regions with great sensitivity, its parameters have not yet been quantified with texture analysis.

The relationship between cerebral veins on SWI and gestational age has been studied in the fetal brain with the number of veins visualized on SWI increasing with gestational age in fetuses [33]. Compared with the brains of preterm infants, the brains of term infants show much more evenly distributed cerebral venous channels [34]. Therefore, at first, we expected entropy, which reflects the irregularity of gray-level distribution, to be higher in preterm infants. However, our results showed higher entropy in term infants compared with that in preterm infants. This could be explained by the denser periventricular venous system of preterm infants compared

with term infants. We drew ROIs to include most DMVs and tried to avoid superficial veins. However, complete exclusion of the superficial veins is not realistically possible. The development of superficial veins in older infants could have resulted in increased entropy. Applying multiple fixed-sized ROIs to the DMVs could be an option to overcome this issue in future studies. We also have to consider that the WM and arterial development itself could have contributed to the increased spatial heterogeneity in infants. For instance, the tortuosity of meningeal arteries increases with age [35].

In our results, skewness decreased with age, from positive values to negative values. When interpreting skewness in our study, the low-intensity DMVs were background signals and relatively high-signal brain parenchyma were highlighted. Skewness suggests asymmetry of the pixel distribution [36]. Positive skewness reflects the predominance of objects brighter than the background and negative skewness reflects predominantly dark objects [36]. The positive skewness in our results can be explained by the brain parenchyma being the

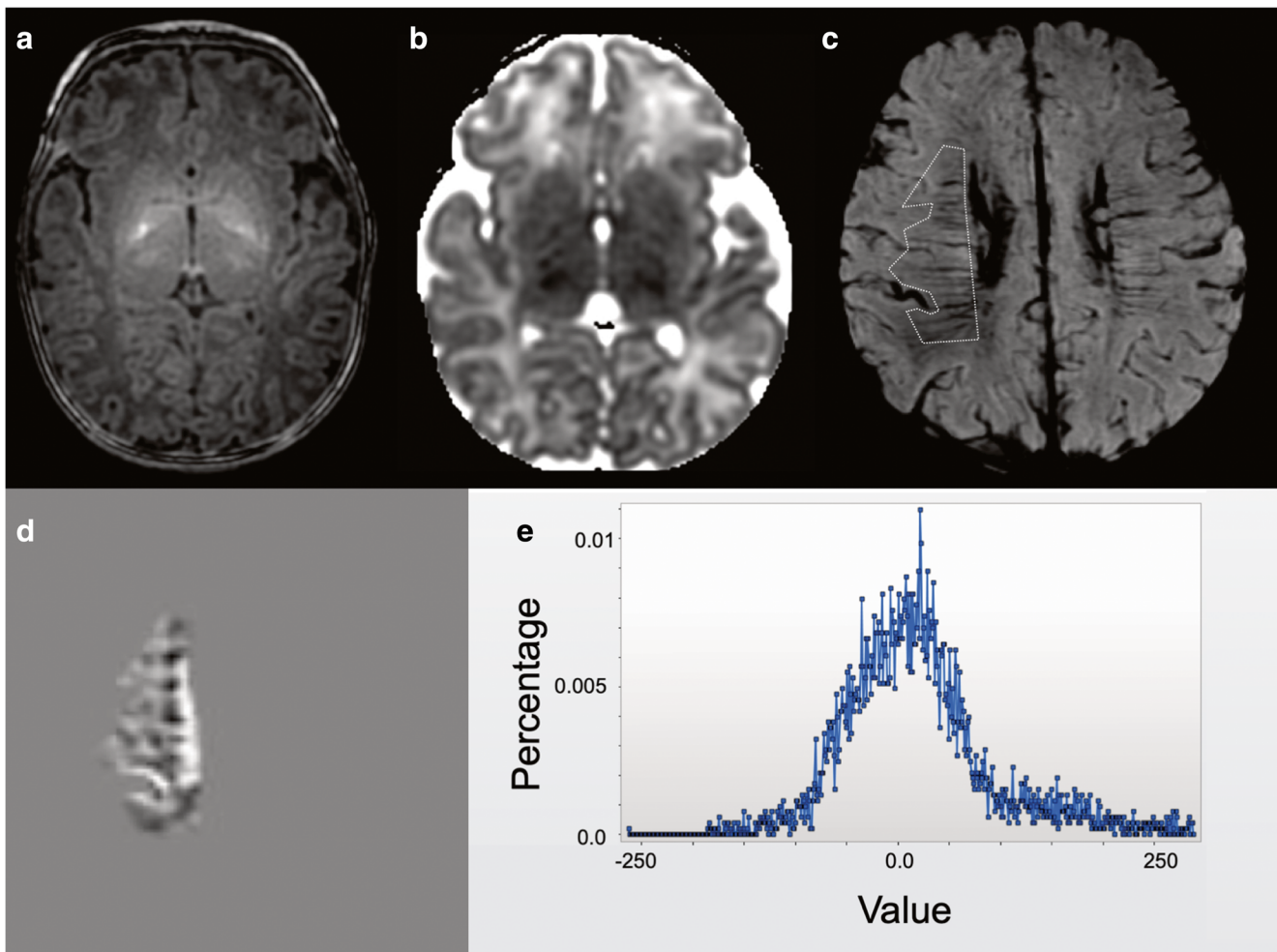


Fig. 4 A full-term infant with asphyxia. T1WI (a), apparent diffusion coefficient map (b), SWI with ROI placement (c), the corresponding texture image (d), and histogram (e) of SWI. Marked T1 high signal changes are noted in the posterior putamen and ventrolateral thalami

(a). Associated apparent diffusion coefficient values are decreased in these regions (b). There is no evidence of focal intracranial hemorrhage, but the DMVs are irregular and engorged (c)

major structure in the ROIs. Decreasing skewness with age could be a result of further development and increased DMV diameters in older subjects.

We know from previous studies that WM injuries can lead to DMV engorgement [7]. Thus, we expected increased entropy in the ischemic group as DMV engorgement will result in irregular appearance. However, entropy did not show significant difference between the normal and ischemic group. On the other hand, skewness was significantly higher in the ischemic group. Increased positive skewness moving away from 0 reflects variation in bright objects. That means two bright objects with different intensities will result in higher skewness than two bright objects with similar intensities. Again, the bright brain parenchyma signal over the dark DMV background could be the key to interpreting this finding. The engorgement of dark DMV over bright brain parenchyma can result in increased variation in bright brain parenchyma signals. Therefore, increased distribution of irregular DMV in the ROIs of the

ischemic injured subjects could lead to higher skewness than normal subjects with even DMV distribution.

One of our study's strengths is the relatively high reproducibility of measurements for entropy and skewness (0.708–0.984) although not for kurtosis (0.189–0.370). Kurtosis was not a significant factor in our results, so low reproducibility of kurtosis was not thought critical. As seen in a previous semi-quantitative evaluation of SWI in children [28], SWI has inevitable low reproducibility, and our results suggest an alternative way of quantifying DMV changes on SWI. Still, its reproducibility should be further validated with a larger number of cases and observations [37].

Although we regarded DMV change as a major factor affecting texture parameters, texture parameters do not differ solely because of DMV changes as the ROIs include the surrounding parenchyma. Parenchymal changes that lead to DWI or T1WI signal changes will inevitably affect texture parameters. However, we think this effect was minimized because of the

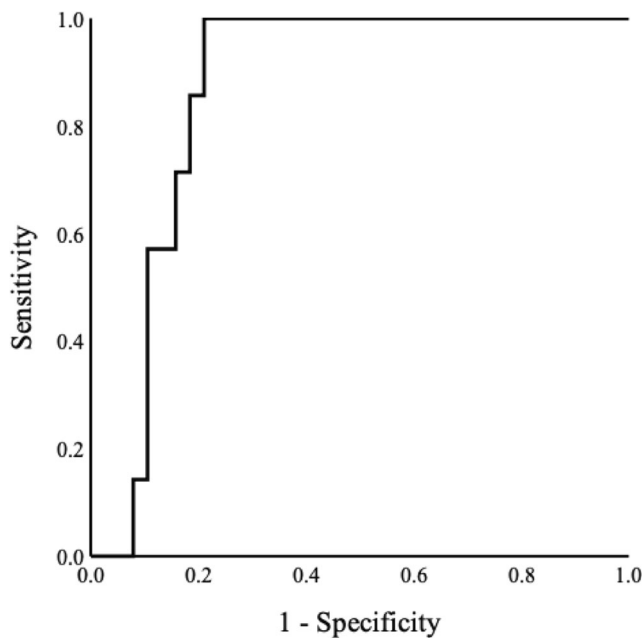


Fig. 5 ROC curve of skewness for differentiating infants with ischemic injury from normal infants

following two reasons. First, we drew ROIs on the minimum intensity projection images of SWI. This postprocessing accentuates the signal intensity loss caused by susceptibility effects and therefore may reduce the effect of the surrounding parenchyma [10]. Second, we selected a spatial scale filter value for the fine texture scale. This filtration step removes image heterogeneity due to noise and highlights biologically important heterogeneity [18]. With selected filtration for fine objects, we accentuated the effect of the fine DMV structure on SWI. In addition, as DMVs were seen as background signals with the brain parenchyma being the major bright object in the ROIs, myelination could have affected the texture parameters according to age. Still, as the ROIs were drawn at the cerebral WM, at which infants in our study population did not yet show myelination signals on MRI [19], the effect of age-related myelination changes to texture parameters is thought to be minor.

Our study has several limitations. Firstly, all patients were scanned with one 3-T MR scanner to minimize variations in image quality. Different magnetic fields or machines for SWI can lead to different signal intensities and other outcomes. With different machines and parameters, preprocessing steps such as bias field correction, pixel spacing, gray-level discretization, and gray-level normalization will increase the robustness of the texture analysis. This is because texture features are sensitive to inhomogeneity [38]. Although we did not perform gray-level intensity normalization, intensity inhomogeneity could have been minimized due to the usage of a single machine in this study. Secondly, only a small number of ischemic injured infants were included. We aimed to investigate the relatively subtle texture difference of DMV changes on SWI without apparent hemorrhagic insult. This is why we excluded many ischemic injured

infants with intracranial hemorrhage. In addition, the MRI manifestation of ischemic injury in these patients was heterogeneous. The degree and stage of ischemia at the time of the MRI scan may have affected the texture parameters. Future studies on this subject are needed to confirm whether SWI texture parameters can be used to show differences in ischemic degree and stage. Also, with a larger number of subjects, it will be possible to make a predictive model for classification purposes. Thirdly, this was a retrospective cross-sectional study. To enhance the clinical impact of these SWI texture parameters, we need to investigate whether they can play a role in predicting neurodevelopment outcomes in infants with ischemia along with other MRI parameters (ex. DWI, DTI, or spectroscopy). In addition, a longitudinal study on this subject will further validate our results in terms of age difference. Lastly, we did not apply intermediate to coarse filtration for texture analysis. It was our belief that fine filtration (2 mm) could better reflect the nature of DMVs rather than spatial scale filter with larger values. Still, applying intermediate to coarse filtration (3–6 mm) could have resulted in further normalization and noise minimization for the robust feature analysis. There are other tools besides TexRAD such as 3D-Slicer [39], IBEX [40], and LIFEX [41] that can be used to extract texture features. We chose to use TexRAD, which is a first-order feature extraction method, because it is easy to implement and has been used before in other MRI studies [42–44]. Unlike some of the other software packages available, TexRAD software does not preprocess images with discretization [45]. Although exploring feature differences between tools or justifying the feature extraction technique of TexRAD is beyond the scope of this paper, extracting the texture features with other filtrations or with other tools will enhance our comprehension on the developmental and ischemic changes of DMVs.

In conclusion, texture analysis on SWI made it possible to quantify DMV information in infants. Entropy increased and skewness decreased with age. Infants with ischemic injury showed higher skewness compared to those without ischemic injury. Although the clinical significance of SWI texture parameters has to be further investigated in a larger number of infants, we suggest that texture analysis on SWI can be a potential tool for identifying infants with ischemic injury.

Acknowledgments The authors thank Hyesun Ko of the Ajou University Hospital for data-gathering.

Funding information This work was partly funded by the National Research Foundation of Korea (NRF-2017R1D1A1B03034768).

Compliance with ethical standard

Guarantor The scientific guarantor of this publication is Hyun Gi Kim.

Conflict of interest The authors of this manuscript declare no relationships with any companies, whose products or services may be related to the subject matter of the article.

Statistics and biometry One of the authors has significant statistical expertise (Hye Sun Lee, Ph.D.).

Informed consent Written informed consent was waived by the Institutional Review Board.

Ethical approval Institutional Review Board approval was obtained.

Methodology

- Retrospective
- Cross-sectional study
- Performed at one institution

References

- Holland BA, Haas DK, Norman D, Brant-Zawadzki M, Newton TH (1986) MRI of normal brain maturation. *AJNR Am J Neuroradiol* 7:201–208
- Volpe JJ (2009) Brain injury in premature infants: a complex amalgam of destructive and developmental disturbances. *Lancet Neurol* 8:110–124
- Li AM, Chau V, Poskitt KJ et al (2009) White matter injury in term newborns with neonatal encephalopathy. *Pediatr Res* 65:85–89
- Krageloh-Mann I, Horber V (2007) The role of magnetic resonance imaging in elucidating the pathogenesis of cerebral palsy: a systematic review. *Dev Med Child Neurol* 49:144–151
- Haacke EM, Mittal S, Wu Z, Neelavalli J, Cheng YC (2009) Susceptibility-weighted imaging: technical aspects and clinical applications, part 1. *AJNR Am J Neuroradiol* 30:19–30
- Sehgal V, Delproposto Z, Haacke EM et al (2005) Clinical applications of neuroimaging with susceptibility-weighted imaging. *J Magn Reson Imaging* 22:439–450
- Arrigoni F, Parazzini C, Righini A et al (2011) Deep medullary vein involvement in neonates with brain damage: an MR imaging study. *AJNR Am J Neuroradiol* 32:2030–2036
- Ramenghi LA, Govaert P, Fumagalli M, Bassi L, Mosca F (2009) Neonatal cerebral sinovenous thrombosis. *Semin Fetal Neonatal Med* 14:278–283
- Kitamura G, Kido D, Wycliffe N, Jacobson JP, Oyoyo U, Ashwal S (2011) Hypoxic-ischemic injury: utility of susceptibility-weighted imaging. *Pediatr Neurol* 45:220–224
- Tong KA, Ashwal S, Obenaus A, Nickerson JP, Kido D, Haacke EM (2008) Susceptibility-weighted MR imaging: a review of clinical applications in children. *AJNR Am J Neuroradiol* 29:9–17
- Ryu YJ, Choi SH, Park SJ, Yun TJ, Kim JH, Sohn CH (2014) Glioma: application of whole-tumor texture analysis of diffusion-weighted imaging for the evaluation of tumor heterogeneity. *PLoS One* 9:e108335
- Eliat PA, Olivie D, Saikali S, Carsin B, Saint-Jalmes H, de Certaines JD (2012) Can dynamic contrast-enhanced magnetic resonance imaging combined with texture analysis differentiate malignant glioneuronal tumors from other glioblastoma? *Neurol Res Int* 2012:195176
- Zhang S, Chiang GC, Magge RS et al (2019) Texture analysis on conventional MRI images accurately predicts early malignant transformation of low-grade gliomas. *Eur Radiol* 29:2751–2759
- Kuijff HJ, Bouvy WH, Zwanenburg JJ et al (2016) Quantification of deep medullary veins at 7 T brain MRI. *Eur Radiol* 26:3412–3418
- Benninger KL, Maitre NL, Ruess L, Rusin JA (2019) MR imaging scoring system for white matter injury after deep medullary vein thrombosis and infarction in neonates. *AJNR Am J Neuroradiol* 40:347–352
- Lee SM, Choi YH, You SK et al (2018) Age-related changes in tissue value properties in children: simultaneous quantification of relaxation times and proton density using synthetic magnetic resonance imaging. *Invest Radiol* 53:236–245
- Huang BY, Castillo M (2008) Hypoxic-ischemic brain injury: imaging findings from birth to adulthood. *Radiographics* 28:417–439 quiz 617
- Skogen K, Schulz A, Dormagen JB, Ganeshan B, Helseth E, Server A (2016) Diagnostic performance of texture analysis on MRI in grading cerebral gliomas. *Eur J Radiol* 85:824–829
- Kim HG, Moon WJ, Han J, Choi JW (2017) Quantification of myelin in children using multiparametric quantitative MRI: a pilot study. *Neuroradiology* 59:1043–1051
- Dean DC 3rd, O’Muircheartaigh J, Dirks H et al (2014) Modeling healthy male white matter and myelin development: 3 through 60 months of age. *Neuroimage* 84:742–752
- Huang YP, Okudera T, Fukusumi A et al (1997) Venous architecture of cerebral hemispheric white matter and comments on pathogenesis of medullary venous and other cerebral vascular malformations. *Mt Sinai J Med* 64:197–206
- Okudera T, Huang YP, Fukusumi A, Nakamura Y, Hatazawa J, Uemura K (1999) Micro-angiographical studies of the medullary venous system of the cerebral hemisphere. *Neuropathology* 19:93–111
- Hooshmand I, Rosenbaum AE, Stein RL (1974) Radiographic anatomy of normal cerebral deep medullary veins: criteria for distinguishing them from their abnormal counterparts. *Neuroradiology* 7:75–84
- Friedman DP (1997) Abnormalities of the deep medullary white matter veins: MR imaging findings. *AJR Am J Roentgenol* 168:1103–1108
- Kersbergen KJ, Benders MJ, Groenendaal F et al (2014) Different patterns of punctate white matter lesions in serially scanned preterm infants. *PLoS One* 9:e108904
- Kocak B, Kizilkilic O, Zeynalova A, Korkmazer B, Kocer N, Islak C (2019) Evaluation of sporadic intracranial cavernous malformations for detecting associated developmental venous anomalies: added diagnostic value of C-arm contrast-enhanced cone-beam CT to routine contrast-enhanced MRI. *Eur Radiol* 29:783–791
- Takanashi J, Suzuki H, Barkovich AJ et al (2003) Medullary streaks: dilated medullary vessels in chronic ischemia in children. *Neurology* 61:583–584
- Meoded A, Poretti A, Benson JE, Tekes A, Huisman TA (2014) Evaluation of the ischemic penumbra focusing on the venous drainage: the role of susceptibility weighted imaging (SWI) in pediatric ischemic cerebral stroke. *J Neuroradiol* 41:108–116
- Young A, Poretti A, Bosemani T, Goel R, Huisman T (2017) Sensitivity of susceptibility-weighted imaging in detecting developmental venous anomalies and associated cavernomas and microhemorrhages in children. *Neuroradiology* 59:797–802
- Messina SA, Poretti A, Tekes A, Robertson C, Johnston MV, Huisman TA (2014) Early predictive value of susceptibility weighted imaging (SWI) in pediatric hypoxic-ischemic injury. *J Neuroimaging* 24:528–530
- Iwasaki H, Fujita Y, Hara M (2015) Susceptibility-weighted imaging in acute-stage pediatric convulsive disorders. *Pediatr Int* 57:922–929
- Polan RM, Poretti A, Huisman TA, Bosemani T (2015) Susceptibility-weighted imaging in pediatric arterial ischemic stroke: a valuable alternative for the noninvasive evaluation of altered cerebral hemodynamics. *AJNR Am J Neuroradiol* 36:783–788
- Dai Y, Dong S, Zhu M, Wu D, Zhong Y (2014) Visualizing cerebral veins in fetal brain using susceptibility-weighted MRI. *Clin Radiol* 69:e392–e397
- Nakamura Y, Okudera T, Hashimoto T (1994) Vascular architecture in white matter of neonates: its relationship to periventricular leukomalacia. *J Neuropathol Exp Neurol* 53:582–589

35. Takashima S, Tanaka K (1978) Development of cerebrovascular architecture and its relationship to periventricular leukomalacia. *Arch Neurol* 35:11–16
36. Miles KA, Ganeshan B, Hayball MP (2013) CT texture analysis using the filtration-histogram method: what do the measurements mean? *Cancer Imaging* 13:400–406
37. Koo TK, Li MY (2016) A guideline of selecting and reporting Intraclass correlation coefficients for reliability research. *J Chiropr Med* 15:155–163
38. Materka A, Strzelecki M (2015) On the effect of image brightness and contrast nonuniformity on statistical texture parameters. *Found Comput Decis Sci* 40:163–185
39. Fedorov A, Beichel R, Kalpathy-Cramer J et al (2012) 3D slicer as an image computing platform for the quantitative imaging network. *Magn Reson Imaging* 30:1323–1341
40. Zhang L, Fried DV, Fave XJ, Hunter LA, Yang J, Court LE (2015) IBEX: an open infrastructure software platform to facilitate collaborative work in radiomics. *Med Phys* 42:1341–1353
41. Orhac F, Soussan M, Maisonobe JA, Garcia CA, Vanderlinden B, Buvat I (2014) Tumor texture analysis in 18F-FDG PET: relationships between texture parameters, histogram indices, standardized uptake values, metabolic volumes, and total lesion glycolysis. *J Nucl Med* 55:414–422
42. Froud R, Palkhi E, Barnfield M, Prestwich R, Vaidyanathan S, Scarsbrook A (2018) Can MR textural analysis improve the prediction of extracapsular nodal spread in patients with oral cavity cancer? *Eur Radiol* 28:5010–5018
43. Makanyanga J, Ganeshan B, Rodriguez-Justo M et al (2017) MRI texture analysis (MRTA) of T2-weighted images in Crohn's disease may provide information on histological and MRI disease activity in patients undergoing ileal resection. *Eur Radiol* 27:589–597
44. De Cecco CN, Ganeshan B, Ciolina M et al (2015) Texture analysis as imaging biomarker of tumoral response to neoadjuvant chemoradiotherapy in rectal cancer patients studied with 3-T magnetic resonance. *Invest Radiol* 50:239–245
45. Larue RT, Defraene G, De Ruysscher D, Lambin P, van Elmpt W (2017) Quantitative radiomics studies for tissue characterization: a review of technology and methodological procedures. *Br J Radiol* 90:20160665

Publisher's note Springer Nature remains neutral with regard to jurisdictional claims in published maps and institutional affiliations.